Characterization of the diastaphenazine/izumiphenazine C biosynthetic gene cluster from plant endophyte *Streptomyces diastaticus* W2

Junli Dong,[1] Beibei He,[1] Ruinan Wang,[1] Xiuli Zuo,[1] Rui Zhan,[1] Linfang Hu,[2] Yiqing Li[2],* and Jing He[1],** (iD)

[1] *State Key Laboratory of Agricultural Microbiology, College of Life Science and Technology, Huazhong Agricultural University, Wuhan, 430070, China.*
[2] *Key Laboratory of Microbial Diversity in Southwest China, Ministry of Education, College of Life Science, Yunnan University, Kunming, 650091, China.*

Summary

Two phenazine compounds, diastaphenazine and izumiphenazine C, with complex structures and promising antitumour activity have been isolated from the plant endophytic actinomycete *Streptomyces diastaticus* W2. Their putative biosynthetic gene cluster (*dap*) was identified by heterologous expression and gene knockout. There are twenty genes in the *dap* cluster. *dap*14-19 related to shikimic pathway were potentially involved in the precursor chorismic acid biosynthesis, and *dapBCDEFG* were confirmed to be responsible for the biosynthesis of the dibenzopyrazine ring, the nuclear structure of phenazines. Two transcriptional regulatory genes *dapR* and *dap4* played the positive regulatory roles on the phenazine biosynthetic pathway. Most notably, the dimerization of the dibenzopyrazine ring in diastaphenazine and the loading of the complex side chain in izumiphenazine C could be catalysed by the cyclase homologous gene *dap5*, suggesting an unusual modification strategy tailoring complex phenazine biosynthesis. Moreover, metabolite analysis of the gene deletion mutant strain *S. albus*::23C5Δ*dap2* and substrate assay of the methyltransferase Dap2

clearly revealed the biosynthetic route of the complex side chain in izumiphenazine C.

Introduction

Natural phenazine compounds are a large class of nitrogen-containing heterotricyclic aromatic alkaloids, mainly produced by *Pseudomonas* and *Streptomyces* species (Laursen and Nielsen, 2004; Mavrodi *et al.*, 2006; Wang *et al.*, 2016; Guttenberger *et al.*, 2017). The dibenzopyrazine core ring is the typical characteristic of all phenazines, while the presence of diverse decorations of functional groups on the core ring system endows them with different physiological roles and broad-specificity biological activities (Mavrodi *et al.*, 2006). Pyocyanin, the best-studied representative of phenazines, has been demonstrated to play an important role in its host, the opportunistic and nosocomial pathogen *Pseudomonas aeruginosa* infection (Lau *et al.*, 2004a,b). The phenazine compounds produced by plant-beneficial *Pseudomonas* spp. not only display antibiotic activities towards plant pathogens, but also contribute to the primary metabolism of phenazine-producing species, including modification of cellular redox states as electron shuttles (Price-Whelan *et al.*, 2007), promotional effects on biofilm formation (Mavrodi *et al.*, 2012) and bacterial survival as cell signals (Dietrich *et al.*, 2008). Although anticancer activities of phenazines have already been discovered since 1959, their application in the development of anticancer and anti-infective agents was trapped due to non-selective DNA intercalation of small phenazine molecules with flatland structures leading to general toxicity (Cimmino *et al.*, 2012). Until the last two decades, dimeric phenazines isolated from *Streptomycete* (such as esmeraldinesA–B (Keller-Schierlein *et al.*, 1989), phenazostatins A–D (Yun *et al.*, 1996; Kim *et al.*, 1997, 1999; Maskey *et al.*, 2003), izumiphenazines A–B (Abdelfattah *et al.*, 2010) and phenazinolin A–E (Ding *et al.*, 2011)) and a few of synthetic and naturally occurring phenazine derivatives bearing a pendant protonatable group were demonstrated to exhibit selective inhibition against tumour cells rather than normal eukaryotic cells, which brings hope for phenazine compounds to be used as clinical drugs (Cimmino *et al.*, 2012). Hence, discovery and characterization of more new

phenazines with complex structures and promising biological activities has attracted new attention recently.

The biosynthetic pathways of simple phenazines have been extensively studied in *Pseudomonas*. Six genes, *phzBCDEFG*, normally organized in one operon, were found to be conserved in all bacterial phenazine biosynthetic gene clusters, and their specific functions in the phenazine core structure biosynthesis have been designated (Mavrodi *et al.*, 2010; Wang *et al.*, 2013; Blankenfeldt and Parsons, 2014), whereafter researchers gradually shift in focus to the study of phenazine-modifying enzymes which are ultimate determinants of distinctive structures and activities. So far, the molecular mechanisms of complex side chain biosynthesis and dimerization of dibenzopyrazine ring were still rarely reported.

The endophytic actinomycete, *Streptomyces diastaticus* W2, isolated from the herb *Artemisia annua*, was found to produce two complex phenazine compounds, diastaphenazine (**1**) and izumiphenazine C (**2**) (Fig. 1), with selective biological activities in our previous article (Li *et al.*, 2015). Besides antibacterial activity against the human pathogen *Staphylococcus aureus*, the newly identified dimeric phenazine diastaphenazine showed extraordinary cytotoxicity against carcinoma cells of human liver, lung, colon, cervix and stomach (Li *et al.*, 2015). Izumiphenazine C contains a phenazine core scaffold attached by an *N*-methyl-para-aminobenzoic acid side chain, which was first identified from the fermentation products of *Streptomyces* sp. IFM 11204 and displayed a synergistic effect with phenazine dimers against human gastric adenocarcinoma (Abdelfattah *et al.*, 2010). In this study, we successfully cloned a phenazine biosynthetic gene cluster from the chromosome of *S. diastaticus* W2 through genome analysis and library construction and demonstrated it responsible for both diastaphenazine and izumiphenazine C biosynthesis. Further functional research of the biosynthetic genes in the cluster disclosed the assembly line of the complex side chain in izumiphenazine C and the possible dimerization pathway to produce diastaphenazine. These results paved the way for elucidation of the biosynthetic mechanisms of complex phenazines and provided the future possibilities for the rational design and modification of phenazine derivatives with antitumour activity based on the combinatorial biosynthesis.

Results and discussion

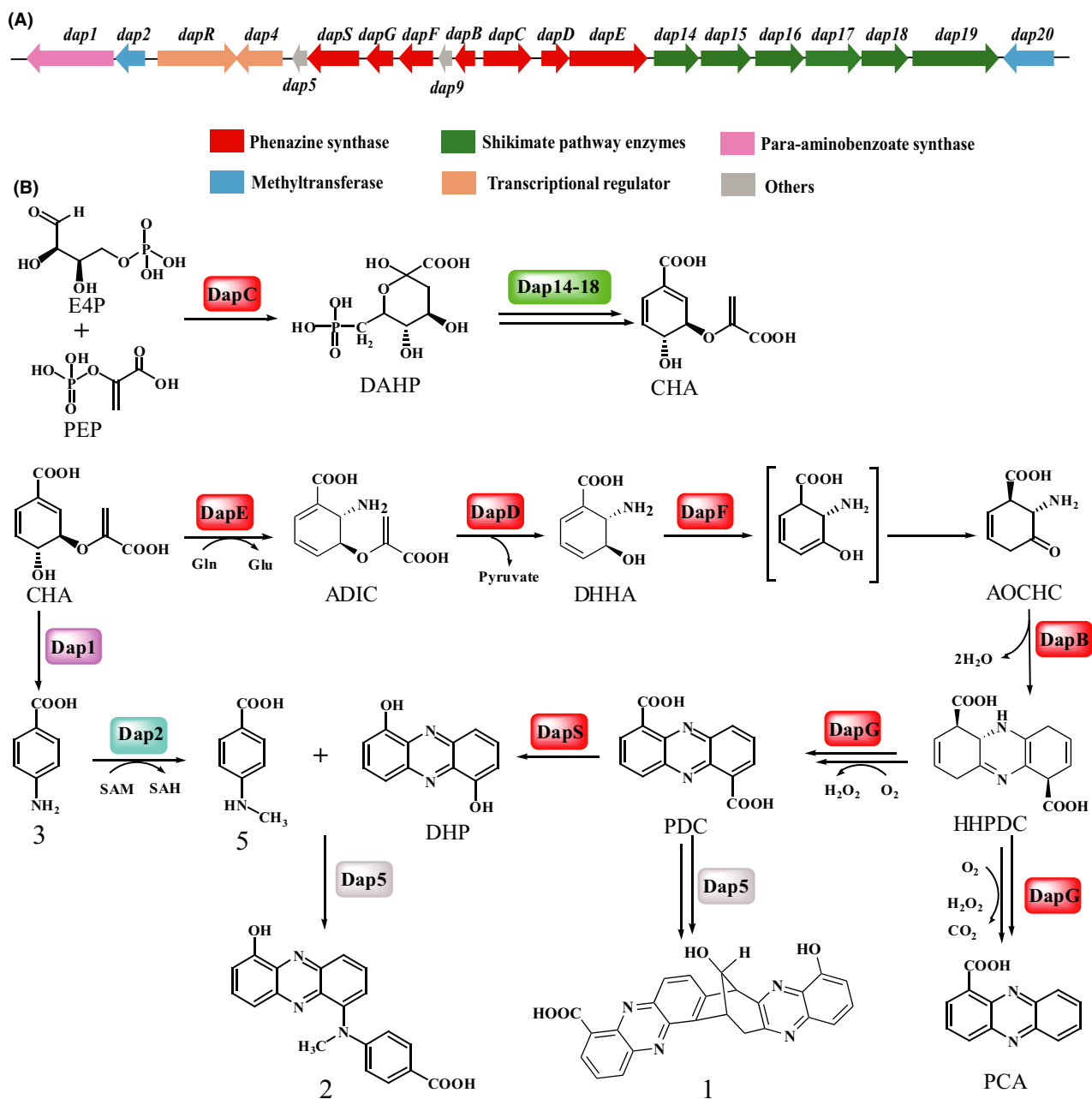### Identification of the diastaphenazine/izumiphenazine C biosynthetic gene cluster

In order to seek out the putative gene cluster responsible for these two complex phenazine-products biosynthesis, the genome DNA of *S. diastaticus* W2 was completely sequenced. A 20 kb-sized gene cluster (*dap*, GenBank accession number MK685983) with 34% homology to the lomofungin biosynthetic gene cluster derived from *Streptomyces lomondensis* (Zhang *et al.*, 2015) was selected out by bioinformatics analysis (Fig. 1A and Table S1). The *dap* cluster consists of 20 open reading frames: 6 shikimate pathway related genes, 6 conserved phenazine biosynthetic genes, 2 regulator genes, 2 methyltransferase genes and several genes with unknown functions.

Further experimental data to authenticate the biological function of *dap* were achieved by construction of the *S. diastaticus* W2 genomic library. The cosmid 23C5 carrying the entire *dap* cluster was screened out from the library and then introduced into *Streptomyces albus* for heterologous expression. High-resolution electrospray ionization mass spectrometry (ESI-HRMS) results showed that the heterologous expression strain *S. albus*::23C5 started to produce the target compounds, diastaphenazine (calcd for *m/z* 437.1254 $[M + H]^+$) (**1**) and izumiphenazine C (calcd for *m/z* 346.1224 $[M + H]^+$) (**2**) as formed by the wild-type producer strain (Fig. 2), while the negative control strain *S. albus*::pMSB carrying the empty vector did not. It is clear that the *dap* cluster possesses requisite genes for the biosynthesis of diastaphenazine and izumiphenazine C.

Regulatory factors

Specific regulatory factors are usually closely aligned with biosynthetic genes. There are two putative regulatory genes, *dapR* and *dap4*, discovered in the *dap* cluster by bioinformatics. DapR, containing a C-terminal helix-turn-helix domain and a PucR superfamily domain, displayed high sequence similarity with the known transcriptional activator AdeR for sporulation of *Bacillus subtilis* (Oudega *et al.*, 1997; Lin *et al.*, 2012). The *dapR* gene was in-frame deleted from the cosmid 23C5 by using λ RED recombination system, and then, the resulting plasmid p23C5Δ*dapR* was introduced into *S. albus* to yield the gene deletion mutant strain *S. albus*::23C5Δ*dapR* (Fig. S1). To exclude the putative polar effect of gene deletion, the entire open reading frame of *dapR* was subsequently cloned into the *Streptomyces* expression vector pWHM4S and introduced into *S. albus*::23C5Δ*dapR* to construct the gene complementation mutant strain *S. albus*::23C5cp*dapR* (Fig. S1). HPLC and ESI-HRMS analyses both revealed the absence of all phenazine compounds including **1** and **2** in *S. albus*::23C5Δ*dapR* and regeneration of them in *S. albus*::23C5cp*dapR* (Figs 2 and S2). Dap4, containing the DDE superfamily motif, shared similarity to *Streptomyces* TylR regulatory proteins (Stratigopoulos *et al.*, 2005). Similar results were obtained in the *dap4* gene knockout and complementation experiments, which demonstrated the positive

(A)

| Phenazine synthase | Shikimate pathway enzymes | Para-aminobenzoate synthase |
| Methyltransferase | Transcriptional regulator | Others |

(B)

Fig. 1. Gene organization of the dap cluster (A) and the proposed biosynthetic pathway (B) of diastaphenazine (**1**) and izumiphenazines C (**2**). E4P: D-erythrose 4-phosphate; PEP: phosphoenolpyruvate; DAHP: 3-deoxy-D-arabinoheptulosonate-7-phosphate; CHA: chorismic acid; ADIC: 2-amino-2-desoxyisochorismate; DHHA: trans-2,3-dihydro-3-hydroxyanthranlic acid; AOCHC: 6-amino-5-oxo-cyclohex- 2-ene-1-carboxylic acid; HHPDC: hexahydrophenazine-1,6-dicarboxylic acid; PCA: phenazine-1-carboxylic acid; PDC: phenazine-1,6-dicarboxylic acid; DHP: 1,6-dihydroxyphenazine; **3**: para-aminobenzoic acid; **5**: 4-methylaminobenzoic acid.

regulatory roles of two regulatory genes in the biosynthesis of phenazines (Figs 2 and S2).

Genes involved in chorismic acid biosynthesis

The shikimate pathway widely distributed in microorganism and plants usually links metabolism of carbohydrates to biosynthesis of aromatic compounds (Dev *et al.*, 2012; Jiang and Zhang, 2016). It is composed of seven enzymatic reactions that convert phosphoenolpyruvate (PEP) and erythrose 4-phosphate (E4P) into chorismic acid (CHA) as the precursor of the aromatic amino acids and many aromatic secondary metabolites. Biosynthesis of phenazines also starts from CHA (Pierson and
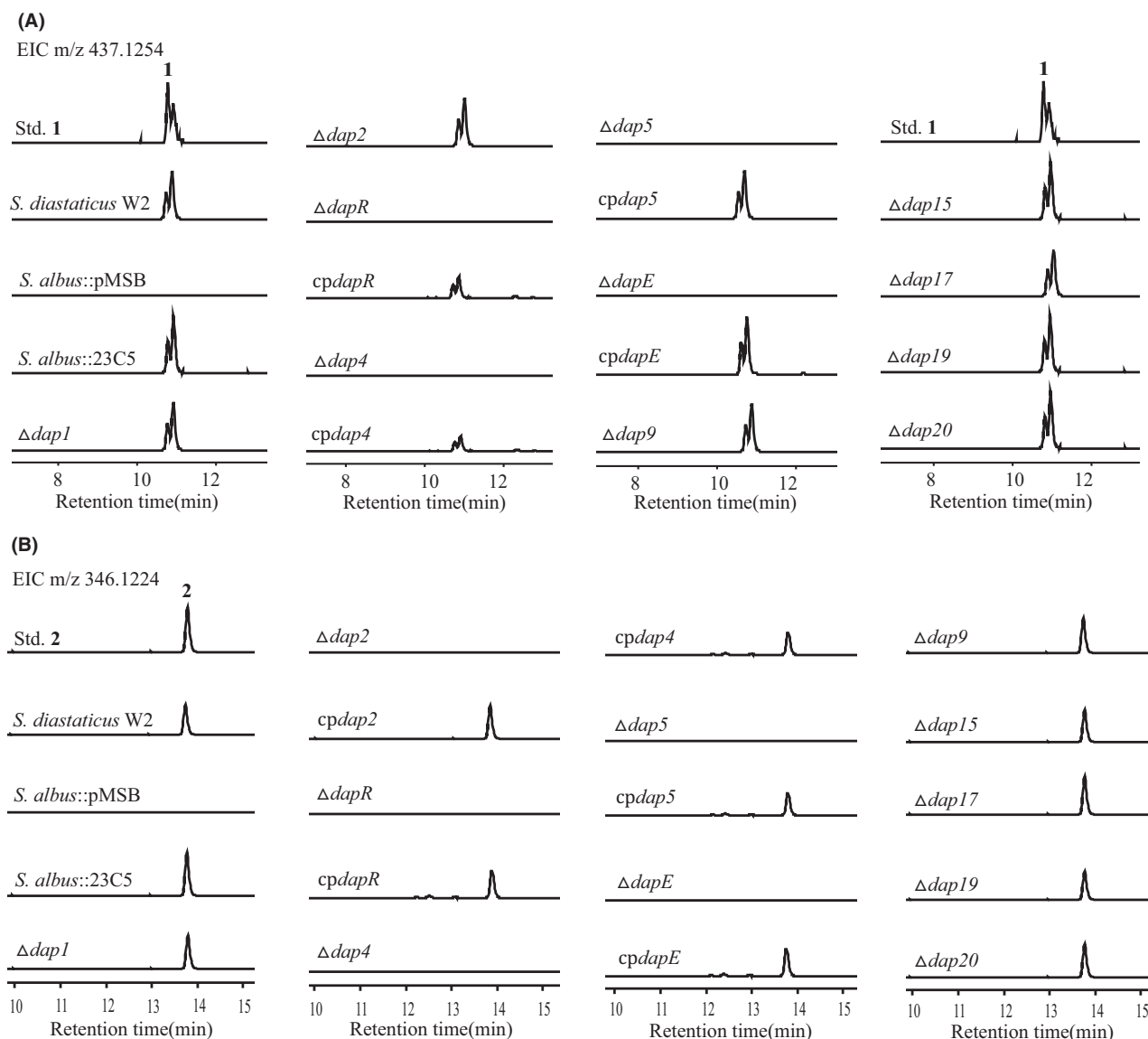
Fig. 2. The EIC traces of diastaphenazine (**1**, *m/z* 437.1254, A) and izumiphenazine C (**2**, *m/z* 346.1224, B) in the heterologous expression strain and mutant strains. *S. diastaticus* W2: wild producer strain; *S.albus*::23C5: heterologous expression strain of the *dap* cluster; *S.albus*::pMSB: heterologous expression strain of the empty vector; Δ*dap1*: *S. albus*::23C5Δ*dap1*; Δ*dap2*: *S. albus*::23C5Δ*dap2*; Δ*dapR*: *S. al-bus*::23C5Δ*dapR*; Δ*dap4*: *S. albus*::23C5Δ*dap4*; Δ*dap5*: *S. albus*::23C5Δ*dap5*; Δ*dapE*: *S. albus*::23C5Δ*dapE*; Δ*dap9*: *S. albus*::23C5Δ*dap9*; Δ*dap15*: *S. albus*::23C5Δ*dap15*; Δ*dap17*: *S. albus*::23C5Δ*dap17*; Δ*dap19*: *S. albus*::23C5Δ*dap19*; Δ*dap20*: *S. albus*::23C5Δ*dap20*; cp*dap2*: *S. albus*::23C5cp*dap2*; cp*dapR*: *S. albus*::23C5cp*dapR*; cp*dap4*: *S. albus*::23C5cp*dap4*; cp*dap5*: *S. albus*::23C5cp*dap5*; cp*dapE*: *S. al-bus*::23C5cp*dapE*.

Pierson, 2010), and thus, a copy of chorismic acid biosynthesis related genes was frequently found in the gene clusters for the biosynthesis of phenazines, e.g. endophenazines from *Streptomyces cinnamonensis* DSM 1042 (Seeger *et al.*, 2011) and esmeraldin from *Streptomyces antibioticus* Tu 2706 (Rui *et al.*, 2012). The same situation occurred in the *dap* cluster.

Bioinformatics analysis showed that Dap19 shared 64% identity with the transketolase Tkt which catalysed

the biosynthesis of erythrose 4-phosphate (E4P), one pre-cursor of the shikimate pathway (Sprenger, 1995). DapC with 55% similarity to 3-deoxy-D-arabinoheptulosonate-7-phosphate (DAHP) synthase PhzC from *Pseudomonas fluorescens* could catalyse the first step of the shikimate pathway (Mavrodi *et al.*, 1998). *dap14*, *dap16* and *dap18* shared high sequence homology with the shikimic path-way related genes *aroA*, *aroC* and *aroB* from *Escherichia coli* respectively. Additionally, Dap17 harbouring two

conserved motifs, shikimate 5-dehydrogenase and shikimate kinase domains, probably exerted dual functions of AroE and AroK. The homolog of AroD (dehydroquinic acid dehydratase) is absent in the *dap* gene cluster. *dap15* homologous with the hydroxylase RdmE gene was found to share the same transcription unit with other shikimate pathway genes and hence speculated to function as AroD in the shikimate pathway. The existence of these genes ensured the precursor supply for phenazine production. However, in-frame deletion of single genes including *dap15*, *dap17* and *dap19*, did not destroy the production of phenazines, but only slightly affected the yield (Figs 2 and S2). Similar result was reported in the esmeraldin biosynthetic research for three shikimic acid pathway related genes *esmA6-A8* as well (Rui *et al.*, 2012). The most likely reason is that the homologous genes involved in the shikimate pathway of primary metabolism took over their duty.

Enzymes for the biosynthesis of dibenzopyrazine ring

Five genes (*dapEDFBG*) in the *dap* cluster were considered to be responsible for the phenazine core formation due to their high sequence similarity with the gene set (*phzEDFBG*) of phenazine biosynthesis in *Pseudomonas* (Biessy and Filion, 2018). As shown in Fig. 1B, *dapE* homologous to the phenazine biosynthetic gene *phzE* was supposed to catalyse the conversion of chorismate acid (CHA) into 2-amino-2-desoxyisochorismate (ADIC) (Mavrodi *et al.*, 1998; Li *et al.*, 2011), which initiated the biosynthesis of phenazine core ring. When the *dapE* gene was in-frame deleted from the cosmid 23C5, the corresponding gene deletion mutant strain *S. albus*::23C5Δ*dapE* lost the capacity for all phenazines production including diastaphenazine, izumiphenazine C and PCA (Figs 2 and S3). The phenazine biosynthetic pathway was resumed once *dapE* was complemented into *S. albus*::23C5Δϖ *dapE* to give rise to the mutant strain *S. albus*::23C5cp-*dapE* (Figs 2 and S3). These results undoubtedly confirmed the critical role of *dapE* in phenazine core production.

DapS implicated in post-modification of phenazine core

The complicated structures of phenazines produced by *Streptomyces* mainly result from more diverse phenazine-modifying enzymes such as the prenyltransferases PpzP, EpzP, Cnqpt1 and Mpz10 (Seeger *et al.*, 2011; Saleh *et al.*, 2012; Zeyhle *et al.*, 2014a,b), the hydroxylase Mpz9 (Zeyhle *et al.*, 2014a), the monooxygenase Lomo10 (Zhang *et al.*, 2015) and the methyltransferases PpzM and EpzM (Seeger *et al.*, 2011; Saleh *et al.*, 2012). In the
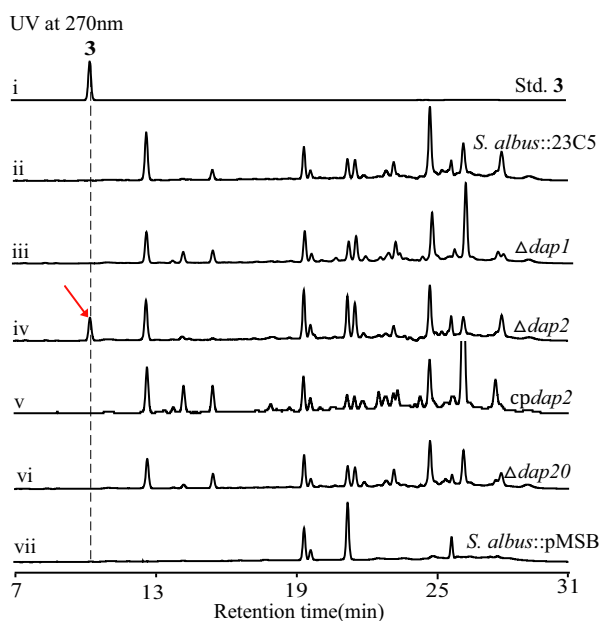
dap cluster, DapS, with high homology to the monooxygenase PhzS from *Pseudomonas aeruginosa* PAO1 and the FMN-dependent monooxygenase XpzG from *Xenorhabdus szentirmaii*, was identified adjacent to the phenazine core biosynthetic genes. PhzS was found to catalyse the oxidative decarboxylation of 5-methylphenazine-1-carboxylate (5-methyl-PCA) to pyocyanine (Stover *et al.*, 2000), while XpzG used PDC as the substrate to form 6-hydroxyphenazine-1-carboxylic acid or 1,6-dihydroxyphenazine under the presence of NADPH or NADH (Shi *et al.*, 2019). In consideration of the chemical structures of diastaphenazine and izumiphenazine C, the function of DapS was supposed to be more similar to XpzG for providing essential precursors for two complex final products. In-frame deletion of the *dapS* gene disrupted the production of diastaphenazine and izumiphenazine C rather than PCA (Fig. S4), verifying its role in the post-modification reactions of phenazine core.

Dap5 is essential for two complex phenazine compounds production

There are two genes, *dap5* and *dap9*, with unknown functions, mingled with the above-mentioned genes. *dap5* encoded a NTF2-like superfamily protein harbouring a snoaL-like polyketide cyclase domain with high homology to an aklanonic acid methyl ester cyclase DauD. Dap9 displayed no similarity to known proteins annotated in NCBI. To investigate whether these two genes involved in phenazine synthesis, their corresponding gene deletion mutant strains *S. albus*::23C5Δ*dap5* and *S. albus*::23C5Δ*dap9* were, respectively, constructed for metabolite analysis. As shown in Figs 2 and S2, deletion of *dap9* had no effect on the biosynthesis of phenazine compounds while the absence of *dap5* abolished the production of diastaphenazine and izumiphenazine C, but PCA and its simple derivatives were still produced (Fig. S3). When the gene *dap5* was complemented into *S. albus*::23C5Δϖ *dap5* to generate the mutant strain *S. albus*::23C5cp-*dap5*, the biosynthesis of diastaphenazine and izumiphenazine C was restored. It is certain that *dap5* has been involved in the biosynthesis of two complex phenazine compounds, rather than in the formation of simple phenazines such as PCA and its derivatives. It was supposed to be the requisite gene critical for the dimerization of the dibenzopyrazine ring in diastaphenazine and the loading of the complex side chain in izumiphenazine C (Fig. 1B). Dap5 belongs to the NTF2-like superfamily whose members are widely distributed in bacteria and exhibit diverse biological functions. The specific catalytic mechanism of this enzyme needs to be explored in the future.

Proposed biosynthetic pathway of izumiphenazine C

Izumiphenazine C has a phenazine core and a para-aminobenzoic acid (PABA) moiety modified by a methyl group. Bioinformatics analysis suggested that the remaining three genes, *dap1*, *dap2* and *dap20*, of the *dap* cluster might be responsible for the *N*-methyl-para-aminobenzoic acid side chain formation of izumiphenazine C. Dap1 shared high sequence similarity to PabS, a para-aminobenzoate synthase widely distributed in microorganisms and plants for conversion of chorismate acid to PABA. Two putative methyltransferase genes, *dap2* and *dap20*, showed high sequence homology to the ribosomal protein L11 methyltransferase protein PrmA and protein-L-isoaspartate O-methyltransferase protein Pcm respectively. Accordingly, Dap1 was supposed to be responsible for the PABA moiety biosynthesis, followed by methylation with the action of Dap2 or Dap20 to render a methyl group to izumiphenazine C. Deletion of the gene *dap1* did not completely abolish the production of izumiphenazine C (Figs 2 and 3), probably because of the generally widespread existence of this kind of genes in microorganisms including the host strain *S. albus*. Meanwhile, two methyltransferase genes deletion mutant strains *S. albus*::23C5Δ*dap2* and *S. albus*::23C5Δ*dap20* displayed totally different results of metabolite analysis. The mutant strain *S. albus*::23C5Δ*dap20* exhibited the same production profile as the original strain *S. albus*::23C5, still producing all phenazines. In contrast, inactivation of *dap2* lost the ability to produce izumiphenazine C, but still produced diastaphenazine (Figs 2 and 3), suggesting that *dap2*, not *dap20*, was involved in the biosynthesis of izumiphenazine C.

A new UV absorption peak was observed in the metabolic analysis of *S. albus*::23C5Δ*dap2* by HPLC (Fig. 3), which was considered to be a crucial intermediate of izumiphenazine C. Large-scale fermentation of the mutant strain *S. albus*::23C5Δ*dap2* was therefore conducted, and two compounds **3** (obsd m/z 138.0641 $[M + H]^+$, calcd for m/z 138.0510 $[M + H]^+$, Fig. S5) and **4** (obsd m/z 332.1024 $[M + H]^+$, calcd for m/z 332.0990 $[M + H]^+$, Fig. S6) were traced. The main intermediate product **3** was identified as PABA through LC-MS/MS and NMR analyses (Figs S7 and S8). However, the isolation of compound **4** was hampered by its low yield. According to the result of ESI-HRMS spectra combined with the putative metabolic pathway, it was proposed to be the demethylated derivative of izumiphenazine C, which had ever been isolated from other phenazine-producing strain and structurally identified in our previous research (Chen *et al.*, 2019). The chemical structure of compound **4** was confirmed by comparative analyses of LC-MS/MS with the previously isolated demethylated izumiphenazine C as the standard (Fig. S9). In the fermentation products of *S. albus*::23C5Δ*dap2*, the newly observed UV absorption peak in HPLC was formed by **3** with high yield, while a trace of **4** could be only detected by ESI-HRMS. Once *dap2* was complemented into *S. albus*::23C5Δ*dap2*, the compounds **3** and **4** disappeared, but izumiphenazine C production was restored (Figs 2, 3 and S10).

Two scenarios are generally conceivable for sequence of the side chain loading and modification in izumiphenazine C: either loading of the PABA moiety prior to methylation modification (route 1) or methylation of PABA prior to loading to phenazine core (route 2) (Fig. 4A). Massive accumulation of PABA (**3**) in *S. albus*::23C5Δ*dap2* significantly supported route 2. Further evidence was provided by *in vitro* enzymatic analysis of Dap2. The gene *dap2* was cloned and overexpressed in *E. coli* (Fig. S11), and the encoded protein was purified for *in vitro* reactions with the compounds **3** and **4** as substrates. In the presence of SAM, PABA (**3**) was completely converted into 4-methylaminobenzoic acid (**5**) by Dap2 in a short period of 2 h, while absence of SAM or inactivated Dap2 resulted in no product formation (Fig. 4B). On the contrary, there was little change in the reaction of **4** incubated with Dap2 and no expected product **2** was detected even if the incubation time was prolonged to
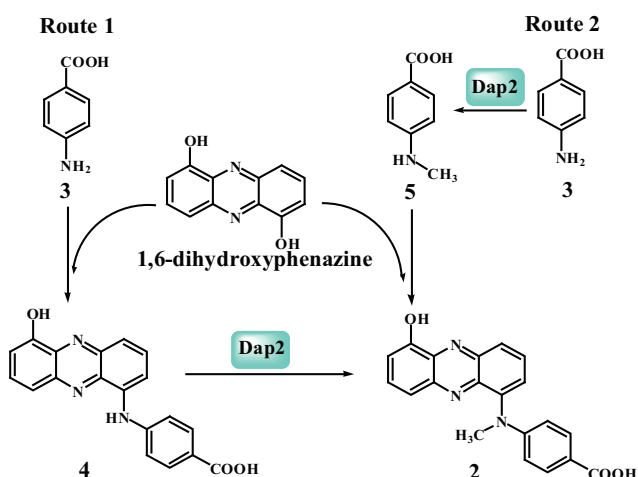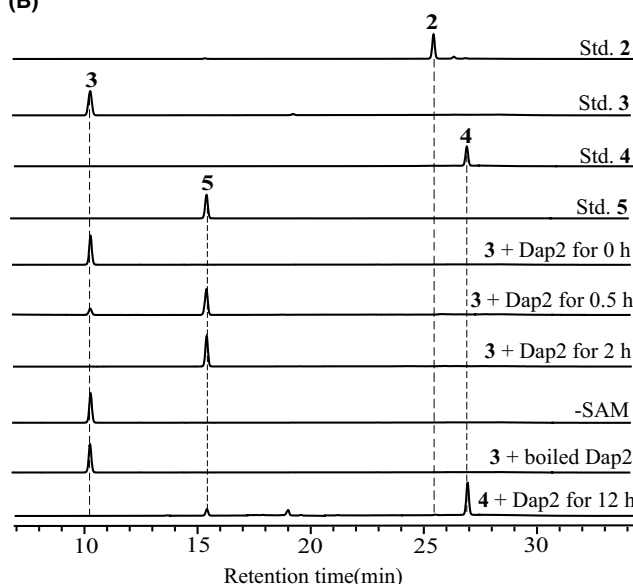

Fig. 3. HPLC analysis of the heterologous expression strain of the *dap* cluster and its mutant strains. **3**: para-aminobenzoic acid; *S.albus*::23C5: heterologous expression strain of the *dap* cluster; *S.albus*::pMSB: heterologous expression strain of the empty vector; Δ*dap1*: *S. albus*::23C5Δ*dap1*; Δ*dap2*: *S. albus*::23C5Δ*dap2*; Δ*dap20*: *S. albus*::23C5Δ*dap20*; cp*dap2*: *S. albus*::23C5cp*dap2*.

(A)

(B)

Fig. 4. Proposed biosynthetic route of the side chain of izumiphenazines C (A) and in vitro substrate analysis of Dap2 (B). **2**: izumiphenazines C; **3**: para-aminobenzoic acid; **4**: strepphenazine C; **5**: 4-methylaminobenzoic acid.

overnight in the same reaction conditions (Fig. 4B). A very small amount of **5** was detected in this reaction system due to spontaneous decomposition of **4** to produce **3** as the substrate of methylation by Dap2. To obtain more direct evidence from *in vivo* experiments, compound **5** was fed to the gene deletion mutant strain *S. albus*::23C5Δ*dap2* and then the result of ESI-HRMS analysis showed the regeneration of izumiphenazine C (Fig. S12). Thus far, all data acquired from *in vivo* and *in vitro* experiments demonstrated that PABA was methylated prior to loading to phenazine core. Broad substrate specificity of the connective enzyme Dap5 might result in the error loading of **3** into the phenazine core to produce traces of **4** in *S. albus*::23C5Δ*dap2*.

Through cloning and functional research of the *dap* cluster from *S. diastaticus* W2, the biosynthetic pathway of two complex phenazines, diastaphenazine and izumiphenazines C, was proposed. It is noteworthy that a few interesting phenazine-modifying reactions were identified, including the dimerization probably catalysed by Dap5 and methylation of PABA by Dap2 to yield 4-methylaminobenzonate for downstream incorporation. Our insights into the biosynthetic pathway of these two compounds not only revealed new modifying enzymes implicated in diversified post-modifications of complex phenazines, but also provided strategies for development of more phenazine drugs by genetic engineering in the future.

Experimental procedures

Bacterial strains, plasmids and growth conditions

The strains and plasmids used in this study were listed in Table S2, and the primers used for PCR were listed in Table S3. All *Escherichia coli* strains including DH5α, BL21(DE3) and S17-1 were grown in LB medium at 37 °C with appropriate antibiotics except that *E. coli* BW25113/pIJ790 was grown in SOB medium at 30 °C. *Streptomyces diastaticus* W2, *Streptomyces albus* and their derivatives were cultivated at 30 °C in TSB medium for DNA extraction and grown on MS medium (2% mannitol, 2% soybean powder, 2% agar) for seed culture and fermentation.

Genome sequencing and bioinformatics analysis

Genomic DNA of *S. diastaticus* W2 was extracted using the standard method (Hopwood *et al.*, 1985). Concentration and quality of DNA samples were determined by using Nanodrop and agarose electrophoresis. The genome of *S. diastaticus* W2 was sequenced by single molecule real-time three generation sequencing technique through PacBio RSII sequencing platform, and the data were assembled by HGAP (hierarchical genome-assembly process) software.

The whole genome sequence of *S. diastaticus* W2 was analysed using antiSMASH (https://antismash.sec ondarymetabolites.org) (Medema *et al.*, 2011) to find putative secondary metabolite biosynthetic gene clusters.

The open reading frames in the newly identified phenazine gene cluster were predicted by using the 2ndFind (http://biosyn.nih.go.jp/2ndfind) and BLASTP (http://blast.ncbi.nlm.nih.gov/Blast.cgi) programs.

Genomic library construction and screening

A genomic library of *S. diastaticus* W2 was constructed according to the previous literature (Li *et al.*, 2008). After genomic DNA was partially digested by Sau3AI, ~40 kb of DNA fragments were recovered using Pulsed Field Gel Electrophoresis (PFGE) and cloned into the BglII site of the vector pMSB152B. The ligation product was packaged by MaxPlax™ Lambda Packaging Extracts (Epicentre) and transfected into the *E. coli* EPI100 to build up a genome library composed of 2400 cosmids. Subsequently, the library was screened by PCR with two pairs of specific primers, 17F1/17R1 and 17F2/17R2.

Heterologous expression of the dap cluster

Five positive cosmids selected out by PCR were then introduced into *S. albus* by intergeneric conjugation for heterologous expression. The corresponding heterologous expression strains were confirmed by PCR.

Gene disruption and complementation

The target gene was deleted from the cosmid 23C5 which contains the entire *dap* cluster, through PCR targeting system (Gust *et al.*, 2003). The streptomycin resistance cassette (*str*) was amplified with a pair of long primers (listed in Table S2) containing 39 nt homology extensions of the target gene at the 5' end and then introduced into *E. coli* BW25113/pIJ790+p23C5 by electroporation. λ RED recombination system promoted replacement of the target gene with the selectable marker *str*, and then, *str* was excised by digestion of the flanking PmeI sites and self-ligation. The resulting plasmid was introduced into *S. albus* by intergeneric conjugation to yield the gene deletion mutant strain.

The target gene cassette containing its complete ORF and RBS was amplified with primers listed in Table S3 and then cloned into pWHM4S. The resulting plasmid was introduced into the corresponding gene deletion mutant by conjugation to obtain the target gene complementation mutant strain. All gene deletion and complementation mutant strains were verified by PCR with primers listed in Table S3.

Fermentation and analysis of phenazine compounds

Streptomyces strains carrying phenazine biosynthetic genes were inoculated on MS medium plates and cultured at 30 °C for 5 days. The solid medium was chopped and extracted with equal volume of ethyl acetate. The crude extract dissolved in methanol was analysed by HPLC using an Agilent 1260 liquid chromatograph system with an Agilent Eclipse Plus C_{18} column (250 × 4.6 mm, 5 μm) at a constant flow rate of 1 ml min^{-1}, with UV detection at 250, 270 and 310 nm. The mobile phase consisted of solvents A (0.1% formic acid) and B (methanol), which were used with the following gradient profile: 0–20 min, 40–90%B; 20–25 min, 90–40%B; and 25–30 min, 40%B. The LC-MS analysis was preformed following the method at a flow rate of 0.4 ml min^{-1} with a linear gradient from 10% to 90% of solvent B in 20 min (solvent A: water/formic acid (999:1); solvent B: acetonitrile/formic acid (999:1)).

Purification of compounds 3 and 4

To isolate and purify compounds **3** and **4**, 20 l fermentation of Δ*dap2* was carried out with MS medium. The crude extract of ethyl acetate was concentrated and loaded onto a column filled with silica gel and flushed with chloroform and different proportions of chloroform–methanol mixture. Outflows were detected by HPLC, and the fractions containing the target compounds were collected. Second purification was conducted on a Sephadex LH20 column with methanol. The purified compounds were finally prepared by semi-preparative HPLC using the same elution method as mentioned earlier.

Expression and purification of Dap2

The encoding gene of Dap2 was amplified from the genomic DNA of *S. diastaticus* W2 using the primers dap2forward/dap2reverse (Table S3). The purified PCR product was cloned into the EcoRI/NdeI sites of the vector pET28a, and the constructed pET-dap2 was then transformed into *E. coli* BL21(DE3) for protein overexpression. The expression of Dap2 fused with His-tag was induced by IPTG and purified by Ni-affinity chromatography.

In vitro *catalytic reaction of Dap2*

The enzyme activity of Dap2 was assayed in a 100 μL reaction system containing 10 μM Dap2, 400 μM substrate (compound 3 or 4), 180 μM SAM and 50 mM Tris buffer (pH 7.8). The reaction mixture was incubated at room temperature for 90 mins and then terminated by mixing 100 μL ethyl acetate. The organic phase was collected and evaporated to dryness. The residue was then dissolved in 100 μL methanol and detected by HPLC and LC-MS analyses.

Conflict of interest

We declare that we have no conflicts of interest.

References

Abdelfattah, M.S., Kazufumi, T., and Ishibashi, M. (2010) Izumiphenazines A-C: isolation and structure elucidation of phenazine derivatives from *Streptomyces* sp. IFM 11204. *J Nat Prod* **73:** 1999–2002.

Biessy, A., and Filion, M. (2018) Phenazines in plant-beneficial *Pseudomonas* spp.: biosynthesis, regulation, function and genomics. *Environ Microbiol* **20:** 3905–3917.

Blankenfeldt, W., and Parsons, J.F. (2014) The structural biology of phenazine biosynthesis. *Curr Opin Struct Biol* **29:** 26–33.

Chen, X., Hu, L.F., Huang, X., Zhao, L.X., and Li, Y.Q. (2019) Isolation and characterization of new phenazine metabolites with antifungal activity against root-rot pathogens of *Panax Notoginseng* from *Streptomyces*. *J Agric Food Chem* **67:** 11403–11407.

Cimmino, A., Evidente, A., Mathieu, V., Andolfi, A., Lefranc, F., Kornienko, A., and Kiss, R. (2012) Phenazines and cancer. *Nat Prod Rep* **29:** 487–501.

Dev, A., Tapas, S., Pratap, S., and Kumar, P. (2012) Structure and function of enzymes of shikimate pathway. *Curr Bioinform* **7:** 374–391.

Dietrich, L., Teal, T.K., Price-Whelan, A., and Newman, D.K. (2008) Redox-active antibiotics control gene expression and community behavior in divergent bacteria. *Science* **321:** 1203–1206.

Ding, Z.-G., Li, M.-G., Ren, J., Zhao, J.-Y., Huang, R., Wang, Q.-Z., *et al.* (2011) Phenazinolins A-E: novel diphenazines from a tin mine tailings-derived *Streptomyces* species. *Org Biomol Chem* **9:** 2771–2776.

Gust, B., Challis, G.L., Fowler, K., Kieser, T., and Chater, K.F. (2003) PCR-targeted *Streptomyces* gene replacement identifies a protein domain needed for biosynthesis of the sesquiterpene soil odor geosmin. *Proc Natl Acad Sci USA* **100:** 1541–1546.

Guttenberger, N., Blankenfeldt, W., and Breinbauer, R. (2017) Recent developments in the isolation, biological function, biosynthesis, and synthesis of phenazine natural products. *Bioorg Med Chem* **25:** 6149–6166.

Hopwood, D.A., Bibb, M., Chater, K.F, Kieser, T., Bruton, C.J., and Kieser, H.M. (1985) *Genetic manipulation of Streptomyces: A Laboratory Manual.* Vol. **56.** Norwich, UK: John Innes Foundation, pp. 388–399.

Jiang, M., and Zhang, H. (2016) Engineering the shikimate pathway for biosynthesis of molecules with pharmaceutical activities in *E. coli*. *Curr Opin Biotech* **42:** 1–6.

Keller-Schierlein, W., Geiger, A., Zaehner, H., and Brandl, M. (1989) Cheminform abstract: metabolites of microorganisms. Part 251. The esmeraldins A and B, dark-green pigments from *Streptomyces antibioticus*, Strain Tue 2706. *ChemInform* **20:** 169–170.

Kim, W.G., Ryoo, I.J., Yun, B.S., Shin-Ya, K., Seto, H., and Yoo, I.D. (1997) New diphenazines with neuronal cell protecting activity, phenazostatins A and B, produced by *Streptomyces* sp. *J Antibiot* **50:** 715–721.

Kim, W.G., Ryoo, I.J., Yun, B.S., Shin-Ya, K., Seto, H., and Yoo, I.D. (1999) Phenazostatin C, a new diphenazine with neuronal cell protecting activity from *Streptomyces* sp. *J Antibiot* **52:** 758–761.

Lau, G.W., Hassett, D.J., Ran, H.M., and Kong, F.S. (2004a) The role of pyocyanin in *Pseudomonas aeruginosa* infection. *Trends Mol Med* **10,** 599–606.

Lau, G.W., Ran, H.M., Kong, F.S., Hassett, D.J., and Mavrodi, D. (2004b) *Pseudomonas aeruginosa* pyocyanin is critical for lung infection in mice. *Infect Immun* **72:** 4275–4278.

Laursen, J.B., and Nielsen, J. (2004) Phenazine natural products: biosynthesis, synthetic analogues, and biological activity. *Chem Rev* **104:** 1663–1686.

Li, L., Xu, Z.N., Xu, X.Y., Wu, J., Zhang, Y., He, X.Y., *et al.* (2008) The mildiomycin biosynthesis: initial steps for sequential generation of 5-hydroxymethylcytidine 5'-monophosphate and 5-hydroxymethylcytosine in *Streptoverticillium rimofaciens* ZJU5119. *ChemBioChem* **9:** 1286–1294.

Li, Q.A., Mavrodi, D.V., Thomashow, L.S., Roessle, M., and Blankenfeldt, W. (2011) Ligand binding induces an ammonia channel in 2-amino-2-desoxyisochorismate (ADIC) synthase PhzE. *J Biol Chem* **286:** 18213–18221.

Li, Y., Han, L.I., Rong, H.E., Li, L., Zhao, L., Wu, L., *et al.* (2015) Diastaphenazine, a new dimeric phenazine from an endophytic *Streptomyces diastaticus* subsp. ardesiacus. *J Antibiot* **68:** 210–212.

Lin, T.H., Wei, G.T., Su, C.C., and Shaw, G.C. (2012) AdeR, a PucR-type transcription factor, activates expression of L-alanine dehydrogenase and is required for sporulation of *Bacillus subtilis*. *J Bacteriol* **194:** 4995–5001.

Maskey, R.P., Kock, I., Helmke, E., and Laatsch, H. (2003) Isolation and structure determination of phenazostatin D, a new phenazine from a marine actinomycete isolate *Pseudonocardia* sp. B6273. *Ztschrift Naturforschung B* **58:** 692–694.

Mavrodi, D.V., Blankenfeldt, W., and Thomashow, L.S. (2006) Phenazine compounds in fluorescent *Pseudomonas* spp. biosynthesis and regulation *. *Annu Rev Phytopathol* **44:** 417–445.

Mavrodi, D.V., Ksenzenko, V.N., Bonsall, R.F., Cook, R.J., and Thomashow, L.S. (1998) A seven-gene locus for synthesis of phenazine-1-carboxylic acid by *Pseudomonas fluorescens* 2–79. *J Bacteriol* **180:** 2541–2548.

Mavrodi, D.V., Parejko, J.A., Mavrodi, O.V., Kwak, Y.S., and Thomashow, L.S. (2012) Recent insights into the diversity, frequency and ecological roles of phenazines in

fluorescent *Pseudomonas* spp. *Environ Microbiol* **15:** 675–686.

Mavrodi, D.V., Peever, T.L., Mavrodi, O.V., Parejko, J.A., Raaijmakers, J.M., Lemanceau, P., *et al*. (2010) Diversity and evolution of the phenazine biosynthesis pathway. *Appl Environ Microbiol* **76:** 866–879.

Medema, M.H., Blin, K., Cimermancic, P., de Jager, V., Zakrzewski, P., Fischbach, M.A., *et al*. (2011) anti-SMASH: rapid identification, annotation and analysis of secondary metabolite biosynthesis gene clusters in bacterial and fungal genome sequences. *Nucleic Acids Res* **39:** W339–W346.

Oudega, B., Vandenbol, M., and Koningstein, G. (1997) A 12 kb nucleotide sequence containing the alanine dehydrogenase gene at 279 degrees on the *Bacillus subtilis* chromosome. *Microbiology* **143:** 1489–1491.

Pierson, L.S., and Pierson, E.A. (2010) Metabolism and function of phenazines in bacteria: impacts on the behavior of bacteria in the environment and biotechnological processes. *Appl Microbiol Biot* **86:** 1659–1670.

Price-Whelan, A., Dietrich, L., and Newman, D.K. (2007) Pyocyanin alters redox homeostasis and carbon flux through central metabolic pathways in *Pseudomonas aeruginosa* PA14. *J Bacteriol* **189:** 6372–6381.

Rui, Z., Ye, M., Wang, S., Fujikawa, K., Akerele, B., Aung, M., *et al*. (2012) Insights into a divergent phenazine biosynthetic pathway governed by a plasmid-born esmeraldin gene cluster. *Chem Biol* **19:** 1116–1125.

Saleh, O., Flinspach, K., Westrich, L., Kulik, A., Gust, B., Fiedler, H.P., and Heide, L. (2012) Mutational analysis of a phenazine biosynthetic gene cluster in *Streptomyces anulatus* 9663. *Beilstein J Org Chem* **8:** 501–513.

Seeger, K., Flinspach, K., Haug-Schifferdecker, E., Kulik, A., Gust, B., Fiedler, H.-P., and Heide, L. (2011) The biosynthetic genes for prenylated phenazines are located at two different chromosomal loci of *Streptomyces cinnamonensis* DSM 1042. *Microb Biotechnol* **4:** 252–262.

Shi, Y.M., Brachmann, A.O., Westphalen, M.A., Neubacher, N., Tobias, N.J., and Bode, H.B. (2019) Dual phenazine gene clusters enable diversification during biosynthesis. *Nat Chem Biol* **15:** 331–339.

Sprenger, G.A. (1995) Genetics of pentose-phosphate pathway enzymes of *Escherichia coli* K-12. *Arch Microbiol* **164:** 324–330.

Stover, C.K., Pham, X.Q., Erwin, A.L., Mizoguchi, S.D., Warrener, P., Hickey, M.J., *et al*. (2000) Complete genome sequence of *Pseudomonas aeruginosa* PAO1, an opportunistic pathogen. *Nature* **406:** 959–964.

Stratigopoulos, G., Bate, N., and Cundliffe, E. (2005) Positive control of tylosin biosynthesis: pivotal role of TylR. *Mol Microbiol* **54:** 1326–1334.

Wang, D.P., Lee, S.H., Seeve, C., Yu, J.M., Pierson, L.S., and Pierson, E.A. (2013) Roles of the Gac-Rsm pathway in the regulation of phenazine biosynthesis in *Pseudomonas chlororaphis* 30–84. *Microbiologyopen* **2:** 505–524.

Wang, D.P., Yu, J.M., Dorosky, R.J., Pierson, L.S., and Pierson, E.A. (2016) The phenazine 2-hydroxy-phenazine-1-carboxylic acid promotes extracellular DNA release and has broad transcriptomic consequences in *Pseudomonas chlororaphis* 30–84. *PLoS One* **11:** e0148003.

Yun, B.S., Ryoo, I.J., Kim, W.G., Kim, J.P., Koshino, H., Scto, H., and Yoo, I.D. (1996) Structures of phenazostatins A and B, neuronal cell protecting substances of microbial origin. *Tetrahedron Lett* **37:** 8529–8530.

Zeyhle, P., Bauer, J.S., Kalinowski, J., Shin-ya, K., Gross, H., and Heide, L. (2014a) Genome-based discovery of a novel membrane-bound 1,6-dihydroxyphenazine prenyltransferase from a marine actinomycete. *PLoS One* **9:** e99122.

Zeyhle, P., Bauer, J.S., Steimle, M., Leipoldt, F., Rösch, M., Kalinowski, J., *et al*. (2014b) A membrane-bound prenyltransferase catalyzes the O-prenylation of 1,6-dihydroxyphenazine in the marine bacterium *Streptomyces* sp. CNQ-509. *ChemBioChem* **15:** 2385–2392.

Zhang, C., Sheng, C., Wang, W., Hu, H., Peng, H., and Zhang, X. (2015) Identification of the lomofungin biosynthesis gene cluster and associated flavin-dependent monooxygenase gene in *Streptomyces lomondensis* S015. *PLoS One* **10:** e0136228.

Supporting information

Additional supporting information may be found online in the Supporting Information section at the end of the article.

Table S1. Deduced functions of genes in the *dap* cluster

Table S2. Bacterial strains and plasmids used in this study

Table S3. Primers used in this study

Fig. S1. Verification of the gene deletion and complementation mutant strains by PCR

Fig. S2. HPLC analysis of metabolite profile of the gene deletion mutant strains

Fig. S3. EIC traces of PCA (*m/z* 225.1513) in the heterologous expression strain and mutant strains

Fig. S4. EIC traces of the compound **1** (*m/z* 437.1254), compound **2** (*m/z* 346.1224) and PCA (*m/z* 225.1513) in the heterologous expression strain and mutant strain

Fig. S5. ESI-HRMS spectra of compound **3**

Fig. S6. ESI-HRMS spectra of compound **4**

Fig. S7. High-resolution LC-MS/MS analysis of the compound **3** (ii) and the para-aminobenzoic acid standard (i)

Fig. S8. ^{1}H NMR (600 MHz, DMSO-d_6) spectrum of compound **3**

Fig. S9. High-resolution LC-MS/MS analysis of the compound **4** (ii) and the demethylated izumiphenazine C standard (i)

Fig. S10. EIC traces of the compounds **3** (*m/z* 138.0641) and **4** (*m/z* 332.1024) in the heterologous expression strain and mutant strain

Fig. S11. SDS-PAGE analysis of the purified Dap2 protein

Fig. S12. LC-MS analysis of the gene deletion mutant strain *S. albus*::23C5Δ*dap2* feeding with compound **5**